Surface transformations on annealed GaAs(001)

C. W. Snyder,* J. Sudijono, Chi-Hang Lam,† M. D. Johnson, and B. G. Orr
The Harrison M. Randall Laboratory of Physics, University of Michigan, Ann Arbor, Michigan 48109-1120
(Received 17 June 1994)

Studies on the surface evolution during vacuum annealing of GaAs(001) have been performed using scanning tunneling microscopy. The transition from an ordered $(2\times4)/c(2\times8)$ reconstructed surface to an ordered mixed phase $(2\times6)/(3\times6)$ reconstruction is observed as the annealing temperature is increased from 450 to 500 °C. The transition to the high-temperature phase is mediated by a transient disordered state. We discuss the origin and role of this state. At higher annealing temperatures, $T\sim520$ °C, in the $(2\times6)/(3\times6)$ phase, we find that terrace edges become unstable, and the surface evolves to a morphology similar to those observed in general pattern-forming systems. A mechanism based on diffusion-limited growth of surface vacancies is discussed.

Understanding surface structure of crystalline semiconductor films is of both technological importance and fundamental interest. The performance of devices fabricated from semiconductor heterostructures is greatly influenced by the quality of interfaces, which in turn is largely determined by surfaces. Annealing, along with other fabrication processes such as etching, passivation, and film growth, significantly affects surface structure. During annealing, the surface evolves via atomistic kinetic processes such as dissociation, diffusion, and desorption. While it is difficult to observe these processes directly, fundamental insight may be obtained from an examination of the structure of surfaces quenched from the annealed state. In this paper we report on scanning tunneling microscopy investigations of GaAs(001) annealed in the temperature range 450–520 °C, *without an arsenic overpressure.* A goal of these experiments was to obtain complimentary real-space information for surface processes previously studied by thermal stimulated desorption-mass spectrometry techniques.[1,2] The transition from a (2×4) reconstructed surface to a mixed phase $(2\times6)/(3\times6)$ reconstruction, and evolution of surface morphology in the $(2\times6)/(3\times6)$ phase were studied.

Experiments were performed in a combined ultrahigh vacuum molecular-beam epitaxy/reflection high-energy electron diffraction (RHEED)/scanning tunneling microscope (STM) system with a base pressure of 1×10^{-10} torr.[3] A feature of this system is the ability to cool samples rapidly (i.e., quench) from elevated temperatures. Samples were prepared by first growing a several thousand angstrom GaAs buffer layer on a GaAs(001) *p*-type (zinc doped) substrate. Homoepitaxial films were then deposited to thicknesses (~120 ML's) at which a dynamical steady state morphology was obtained.[4] The film morphology at different stages of growth has been previously investigated.[5,6] Upon stopping homoepitaxial growth, it was useful to control "recovery" of the surface. Recovery refers to the process whereby surface roughness, at the time of growth interruption, decreases as the surface is annealed at growth temperature in an arsenic ambient. There is a corresponding increase in intensity of the specularly reflected RHEED beam during this process, and the surface is considered "recovered" when the specular beam intensity reaches a maximum. A variety of different initial surface morphologies could be obtained by varying the length of recovery time from seconds [this produces what we describe as an "unrecovered" surface; see Fig. 3(a) and Ref. 6], to tens of minutes, for a recovered surface [see Fig. 2(a)].

For the studies discussed here, the initial film surface was first imaged by STM, then inserted into the growth chamber for annealing. Reflection high-energy electron diffraction was used to monitor surface evolution in real-time during annealing, and upon quenching, comparative STM imaging was performed. Annealing temperatures ranged from 450–520 °C, as measured by infrared pyrometry, and were well below the congruent sublimation point ($T=640$ °C) (Ref. 7) and high temperatures ($T=670$ °C) previously used to investigate layer-by-layer evaporation.[8] Ambient arsenic pressures remained in the low 10^{-10}-torr range (i.e., "vacuum annealing"), and residual arsenic adsorption during sample cool down and transfer to the STM was neglible. Vacuum annealing, quenching, and STM imaging were performed iteratively for several days on a surface without significant degradation due to contamination.

For our experiments, vacuum annealing was initiated at temperatures between 450–480 °C, as below $T=450$ °C, measurable changes were not observed by RHEED on a time scale of tens of minutes. For *all* samples, independent of the initial surface morphology, in less than 1 min of annealing, the RHEED patterns changed from rather sharp $2\times4/c(2\times8)$ patterns, indicative of well-ordered surfaces, to rather diffuse 1×1 patterns, indicative of disordered surfaces. Increasing the temperature to 520 °C over a period of several minutes converted the surface to a fairly well-ordered mixed phase $(2\times6)/(3\times6)$ reconstruction. STM images of surfaces corresponding to each of the phases observed by RHEED are shown in Figs. 1(a)–1(c). Figure 1(a) displays the typical $2\times4/c(2\times8)$ reconstructed surface,

 ©1994 The American Physical Society

and the surface structure in Fig. 1(c) has been discussed in Ref. 9. The surface of Fig. 1(b) is of interest here, and is discussed below. Although there was evidence from RHEED for some weak transitory phases (1×6, 6×6, 4×6), as has been observed by others,[10–12] we find the final, stable surface reconstruction at $T=520\,^{\circ}\mathrm{C}$ is the mixed phase $(2\times6)/(3\times6)$. The mixed 2×6 and 3×6 symmetry is consistent with previous LEED results and in partial agreement with previous STM results.[9] We reemphasize that evolution of the RHEED pattern dur-

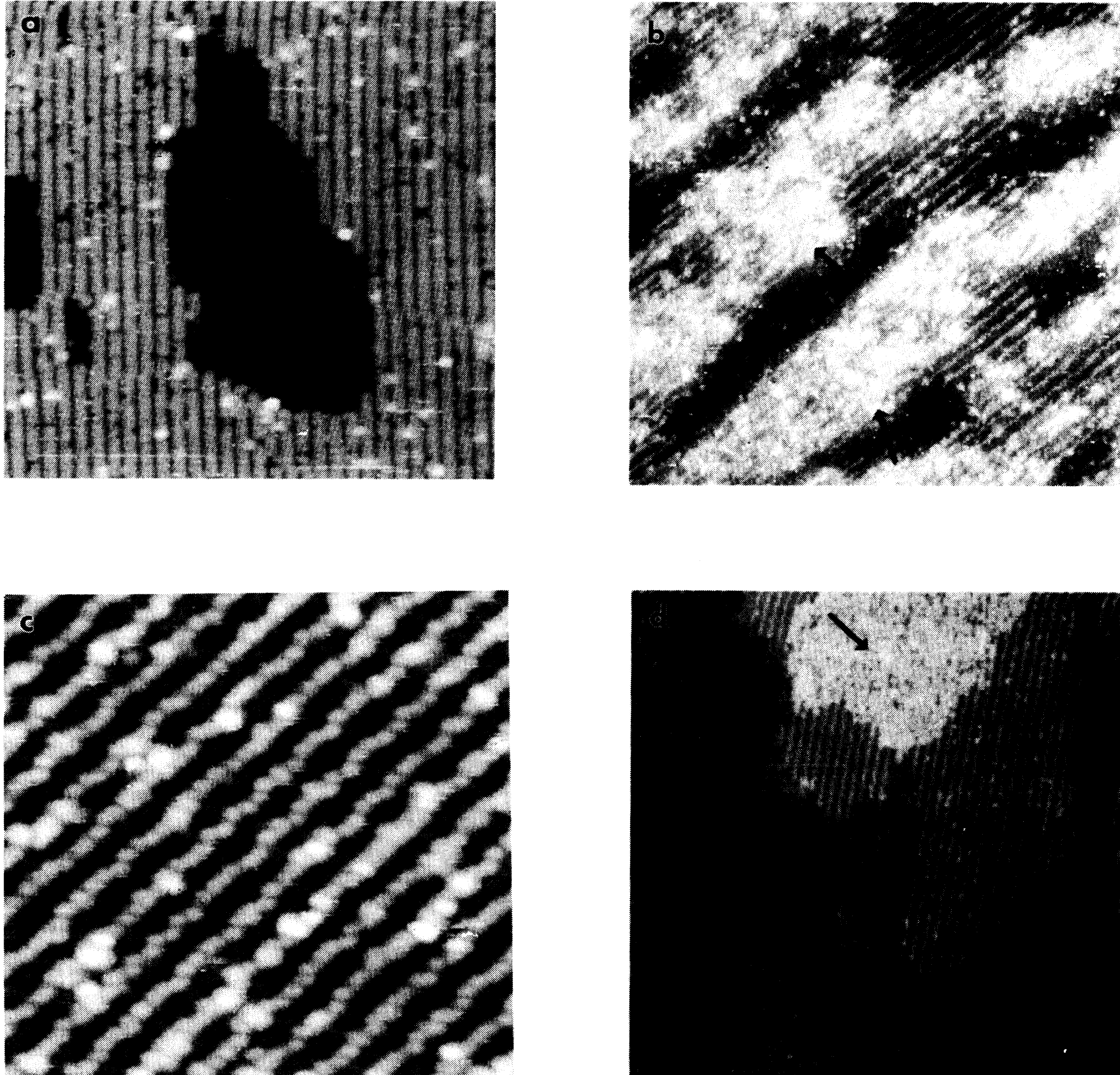

FIG. 1. Note: The orientation of the surface crystallographic directions in the figures is not necessarily the same for each figure because of rotation of the STM during the "course approach" and retraction. For all STM images, the sample bias voltage was +2.6 V and the tunneling current was 60 pA. All steps in STM images are an atomic bilayer, 0.28 nm in height. (a) High-resolution STM image of the $(2\times4)/c(2\times8)$ reconstructed GaAs(001) surface. All surfaces prior to annealing displayed this reconstruction. The scan range is 35×35 nm^2. (b) High-resolution STM image of a vacuum annealed ($T\sim480\,^{\circ}\mathrm{C}$) surface which was quenched in the intermediate disordered state. The scan range is 60×60 nm^2. This image displays nucleation of the $\times6$ phase from the disordered surface. The atomically disordered regions (indicated by arrows) have a fuzzy texture and are believed to be made up of arsenic (i.e., arsenic clusters), while the ordered rows correspond to $\times6$ regions. (c) High-resolution STM image of the $(2\times6)/(3\times6)$ reconstructed surface. The scan range is 20×20 nm^2. (d) STM image of vacuum annealed unrecovered surface in the $(2\times6)/(3\times6)$ phase which was quenched prior to reaching the steady state fingerlike morphology. The scan range is 80×80 nm^2. The image was obtained near a ragged terrace edge and displays disordered 2D clusters absent of arsenic dimers. These 2D clusters (indicated by arrows) are believed to be Ga rich.

ing vacuum annealing was qualitatively the same for unrecovered initial surfaces [which have a relatively high step-edge density, see Fig. 3(a)] and recovered initial surfaces.

Thermal desorption experiments previously demonstrated that it is primarily As_2, and to a much lesser extent, Ga, which desorbs when GaAs(001) is flash heated without an arsenic overpressure in the temperature range 300–600 °C.[1,2] In addition, observations by electron diffraction of a (2×4) to $\times6$ structural transition during vacuum annealing have been reported.[9–12] From the earlier work, it can be concluded that the arsenic surface coverage for any of the $\times6$ phases is reduced relative to the (2×4) phase, and that during the transition from the (2×4) to the $(2\times6)/(3\times6)$, the arsenic surface coverage is reduced by approximately 0.5 ML.[1,13] The remainder of the arsenic apparently participates in the formation of the $(2\times6)/(3\times6)$ phase. Based on these previous studies, it is expected that the $\times6$ phases (the transitory phases or the stable phase) nucleate directly from the (2×4) phase. In contrast, our results indicate that nucleation occurs from an intermediate disordered state characterized by a diffuse 1×1 RHEED pattern. We note, that if the temperature is increased rapidly up to 520 °C, this state only appears for a few seconds, and is likely to be missed altogether; perhaps explaining why it has not been reported. Additionally, if the sample is slowly cooled down from the $(2\times6)/(3\times6)$ in a slight arsenic ambient, in order to form the 2×4 phase, there is little or no evidence of it; the transition to the 2×4 reconstruction occurs very quickly. Nevertheless, by annealing slowly without an arsenic ambient the disordered state persists for several minutes. We have quenched the surface at an early stage in the formation of the $\times6$ phase from the disordered state. This is shown in STM images of Figs. 1(b) and 2(b). The RHEED pattern associated with Fig. 1(b) had faint $\times6$ steaks superposed on the diffuse 1×1 pattern. There is consistency between the atomic scale features in Fig. 1(b) and the RHEED pattern, as we associate diffuseness in the RHEED pattern with the atomically disordered regions, the $\times6$ streaks with the ordered patches between disordered regions, and the 1×1 features with "bulk" diffraction. We rule out the possibility that the majority of diffuse scattering arises from large-scale structure (i.e., step-edge scattering) by noting that atomically ordered surfaces with equal or greater step-edge density had significantly less diffuseness in the RHEED pattern. Thus, the atomically disordered regions give rise to the majority of diffuse scattering.

Although not conclusive, STM suggests that the disordered regions of the surface are made up of arsenic. This is established through a comparison of the disordered regions in Fig. 1(b) with the more resolved disordered two-dimensional (2D) clusters in Fig. 1(d). Figure 1(d) was obtained after vacuum annealing at 520 °C an unrecovered initial surface. It is relevant here for comparison purposes. While the image in Fig. 1(b) was obtained from the middle of a large terrace, Fig. 1(d) was obtained from a ragged edge of a terrace after slightly higher temperature vacuum annealing, in order to desorb the disordered "arsenic" and produce the $(2\times6)/(3\times6)$ phase (note: the anneal was not of sufficient length of time to form fingering patterns—see discussion below). We have observed that nucleation of the $(2\times6)/(3\times6)$ phase is affected by surface morphology. In particular, we find an almost complete lack of arsenic dimer formation on small 2D islands and near the edges of peninsula-shaped terraces, thus we expect an arsenic deficiency in these regions. Arrows in Fig. 1(d) indicate these regions: they appear as disordered 2D clusters, on which there is apparently no arsenic dimer formation, extending out from arsenic dimerized regions which are $(2\times6)/(3\times6)$ reconstructed. These clusters are very likely made up of disordered Ga. Since the disordered regions in Fig. 1(b) have a distinctive texture markedly different from the supposed Ga clusters in Fig. 1(d), we speculate the disordered regions in Fig. 1(b) are mostly made up of arsenic.

The intermediate disordered state is of primary interest for insight into atomistic processes involved in the transition between the stable (2×4) and $(2\times6)/(3\times6)$ phases. We speculate on its nature by considering known processes occuring during GaAs *growth*. It is widely accepted that in the growth of GaAs using molecular arsenic source (As_2 or As_4), upon arrival at the surface a molecular precursor state, made up of physisorbed As_2, forms.[7] Incorporation then proceeds via dissociative chemisorption into vacant As sites at the surface, typically forming the As-stabilized (2×4) phase. Previous thermal-desorption studies, which found that arsenic primarily desorbs as As_2, suggest that during annealing without an arsenic overpressure, arsenic desorption occurs through the reverse process: arsenic atoms from surface sites recombine into As_2, forming a physisorbed molecular state, and from this weakly bound configuration, As_2 desorption takes place.[1,2] Thus, it is reasonable that the disordered "arsenic" regions in Fig. 1(b) are made up of arsenic molecules that were quenched from the precursor state. As mentioned above, this state does not appear when cooling in the presence of an arsenic ambient in order to pass from the $(2\times6)/(3\times6)$ phase to the (2×4) phase. For the transition, $(2\times6)/(3\times6)\rightarrow(2\times4)$, in which the arsenic surface coverage increases, arsenic is being supplied from the vapor phase flux and the kinetic processes for forming the (2×4) phase are apparently rather fast. On the other hand, for the transition, $(2\times4)\rightarrow(2\times6)/(3\times6)$, we observe the kinetic processes to be relatively slow. It appears then that the role of the intermediate disordered state is as a kinetically preferred configuration from which desorption occurs and the formation of the $(2\times6)/(3\times6)$ phase is facilitated.

We now turn to observations of the large-scale surface structure (i.e., morphology) of vacuum annealed surfaces. Of particular interest are the intriguing fingering patterns shown in Figs. 2(c) and 3(b). Figure 2 reveals the evolution of the film morphology from the $(2\times4)/c(2\times8)$ reconstructed recovered surface [Fig. 2(a)], to a surface covered with the disordered arsenic layer [Fig. 2(b)], discussed above, to a very striking fingering pattern on the $(2\times6)/(3\times6)$ reconstructed surface [Fig. 2(c)], as the sample is heated from $T=480$ to 520 °C. While the surface morphology shown in Fig. 2(c) was obtained after

vacuum annealing a relatively smooth (i.e., low step-edge density), recovered initial surface, the pattern in Fig. 3(b) was obtained after vacuum annealing a rather "rough" (i.e., high step-edge density) unrecovered initial surface, as in Fig. 3(a). Thus, it seems that production of fingering patterns is somewhat independent of initial surface morphology. Samples were typically heated for several minutes at $T=520\,^{\circ}\mathrm{C}$ in order to form such patterns, and the surfaces were always $(2\times6)/(3\times6)$ reconstructed.

The surface morphology in Figs. 2(c) and 3(b) is reminiscent of shapes observed in a wide variety of pattern forming systems, such as dendrite solidification, viscous fingering in liquid systems, electrochemical deposition, and dielectric breakdown.[14] Such systems are representative of far from equilibrium growth in the diffusion limited regime. Growth in this regime is principally characterized by an unstable interface.[15] Such instabilities can lead to complex disorderly fractal structures as well as highly symmetric and regular pattern morphologies.[14] Based on the strong resemblance of our images to morphologies produced in well known pattern forming systems, we speculate that diffusion limited growth is controlling the surface evolution.

We first consider other investigations of surface insta-

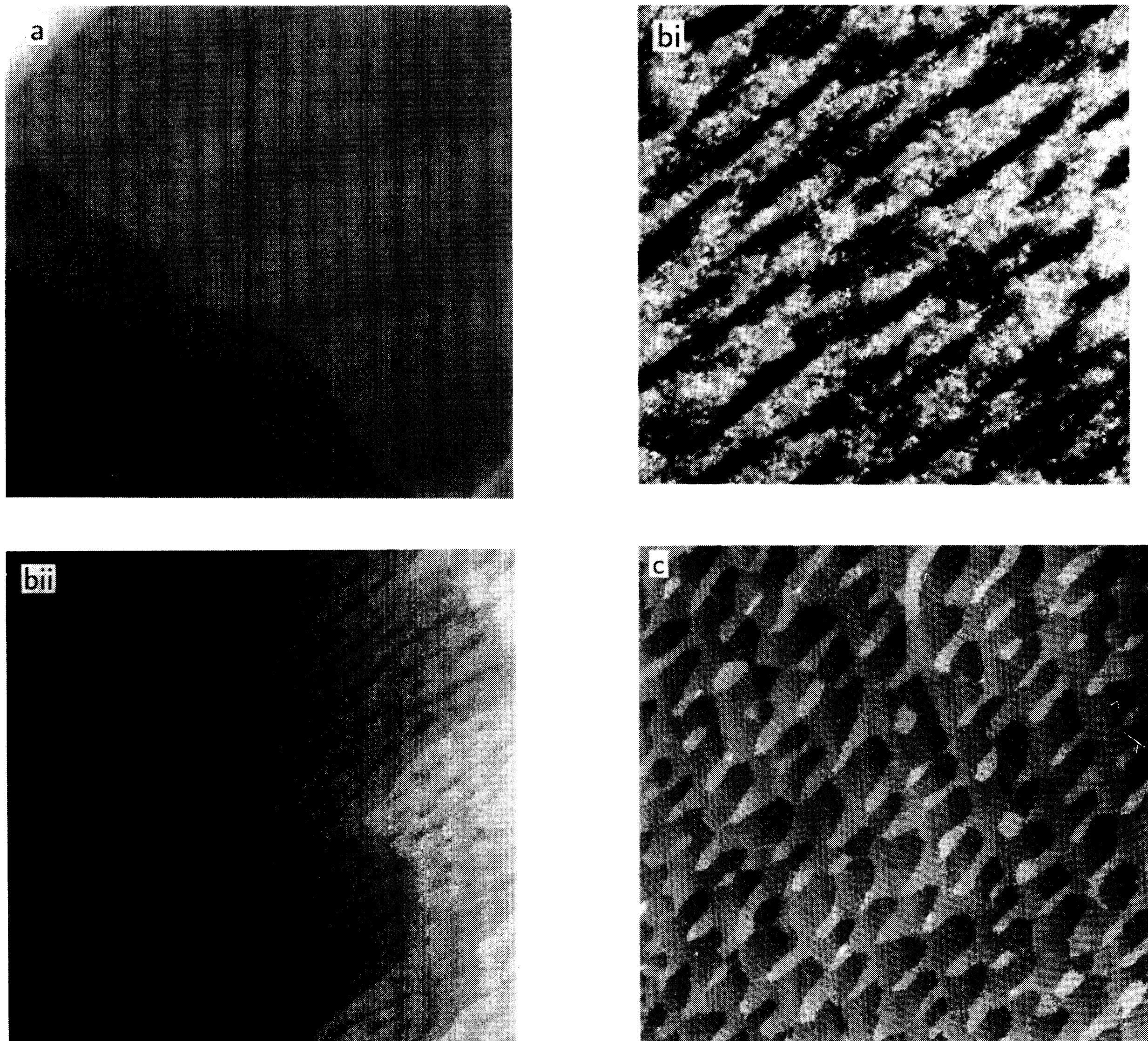

FIG. 2. (a) STM image of a recovered initial surface. The terrace edges run along the [110] direction. The scan range is 400×400 nm^2. (b) STM images after vacuum annealing a recovered surface to $\sim480\,^{\circ}\mathrm{C}$ and quenching in the intermediate disordered state. The scan range for the small scale image (bi) is 150×150 nm^2. The scan range for the large scale image (bii) is 400×400nm.^{2} The RHEED pattern for these surfaces was a 1×1 diffuse pattern with faint $\times6$ streaks superposed. (c) STM image of fingering patterns produced by vacuum annealing a recovered surface. The scan range is 1×1 μm^2. The fingerlike features point in the $[\bar{1}10]$ direction. The circular fringelike pattern is an artifact caused by a loose tip.

bilities as they relate to possible mechanisms of diffusion and growth in our experiments. Previously, a terrace-edge instability during vapor deposition was proposed,[16] and fractal-like patterns created through deposition were observed.[17] In those earlier studies, instabilities occurred through adatom surface diffusion and growth at terrace edges. Observations in our annealing experiments are distinct from earlier studies in that deposition is not occuring. During annealing, on the other hand, instabilities are not expected; capillary induced smoothing of terrace-edges via adatom diffusion is more likely in order to lower surface free energies (e.g., Si).[18] Indeed, capillary-induced smoothing of GaAs annealed in an arsenic ambient quite likely provides the mechanism for the well-known surface recovery phenomenon. Surprisingly, however, we demonstrate that upon annealing GaAs ($T = 520\,^{\circ}$C) *without* an As ambient, the surface becomes unstable. It seems quite improbable that the instability occurs through some process of correlated surface diffusion of Ga and As adatoms to terrace edges. In addition, an uncorrelated process, in which a Ga adatom diffuses to a terrace edge and then is chemisorbed to by an independent As, also seems implausible without an As ambient.

We consider the idea that surface vacancies, created on terraces by desorption or detachment during annealing, are the "active" species responsible for the surface evolution. Recently, a picture has emerged in which surface vacancies may be viewed as diffusion adparticles analogous to mobile adatoms in film deposition. This is based, in part, on experiments investigating surface vacancy mediated changes to surface structure and morphology.[19,20] In these studies, two-dimensional nucleation of vacancy clusters and layer-by-layer material removal via surface vacancy creation were reported. For the GaAs surface, we expect the adparticle to be either an arsenic vacancy or an As/Ga vacancy. Since arsenic vacancy diffusion is a one-particle process, and As/Ga vacancy diffusion is a two-particle process, we expect the former to be more probable. During the formation of the instability, both arsenic and gallium atoms are displaced from their initial surface sites. The displaced arsenic desorbs and the displaced Ga perhaps desorbs slowly or forms widely separated Ga clusters with a spacing much larger than the STM field of view. We have not observed Ga clusters after fingering patterns were formed. However, we do observe Ga coating of the terrace edges (see Fig. 4).

A natural mechanism by which surface vacancies could produce the instabilities displayed in Figs. 2(c) and 3(b) is diffusion limited growth at a terrace edge. This is directly analogous to diffusion limited growth of adatoms at a terrace edge during step-flow growth, discussed by Bales

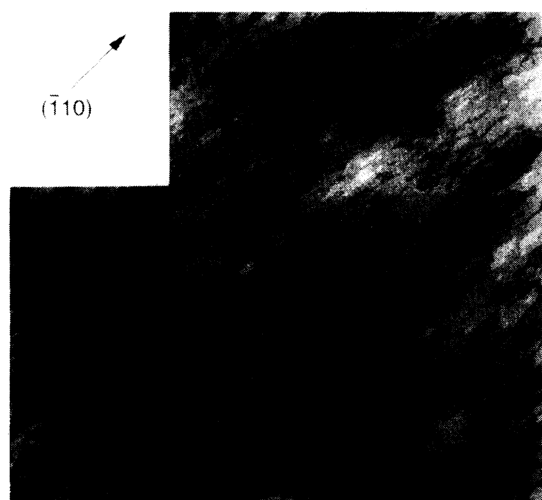

FIG. 3. (a) STM image of an unrecovered initial surface. The scan range is 600×600 nm^2. (b) STM image of fingering patterns produced by vacuum annealing an unrecovered initial surface. The scan range is 750×750 nm^2. The fringelike pattern is an artifact caused by a loose tip.

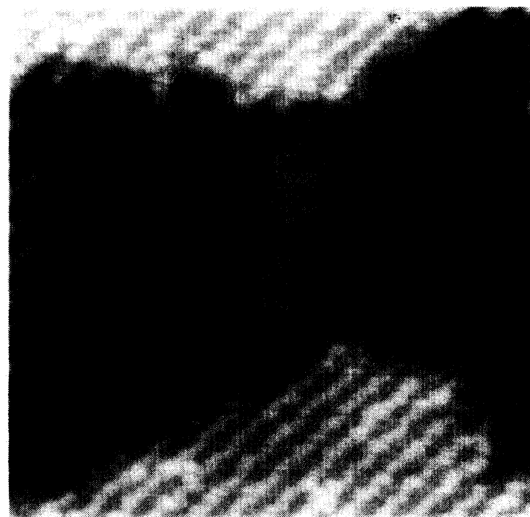

FIG. 4. STM image showing Ga coating of terrace edges on a surface displaying the fingering patterns. The scan range is 35×35 nm^2. Although, not apparent from the gray level display of the image, a measurable weight difference exists between the arsenic dimers on the lower terrace and the Ga which coats and connects the two upper terrace edges.

and Zangwill.[16] If the analogy is to hold for surface vacancies, a boundary condition of unequal attachment rates at the terrace edge should be physically valid and the steady-state concentration of vacancies on the terrace should obey the diffusion equation. Just as adatom attachment rates are expected to be asymmetric,[21] it also appears likely that vacancy attachment rates are asymmetric. The step energy is likely to play a role, and Ga coating of the normally As-terminated steps (see Fig. 4) may alter the step energy so that vacancy attachment rates from above and below are unequal. Indeed, unstable terrace edges have recently been observed in a two-component system whereby one species diffuses to the terrace edges and passivates the steps.[22] The conditions under which the diffusion equation is appropriate are twofold: the concentration of vacancies is not highly supersaturated (i.e., 2D vacancy islands do not nucleate on the terrace) and there is an energetic preference for vacancies to migrate to a step. The former is controlled by substrate temperature, and from simple bond counting arguments, the latter is quite reasonable.

Given that the terrace edge instability we observe is representative of a diffusive instability, the characteristic wavelength shown in Figs. 2(c) and 3(b) may be naturally understood as a competition between capillary-induced smoothing and the diffusion field of vacancies bounding the step. The lack of tip splitting and side branches might be expected from anisotropy in the surface tension (i.e., step energies). Indeed, for GaAs (001) the step energy for [110] is higher than $[\bar{1}10]$.[23] It should be mentioned that we do not observe single isolated vacancies, perhaps this is because vacancies have sufficient mobility to reach a terrace edge during quenching. Nevertheless, we observe small 2D vacancy clusters.

In summary, the data presented here reveals that the (2×4) to $(2\times6)/(3\times6)$ phase transition is not direct, in contrast to expectations based on earlier work.[10–12] We have shown that there is a kinetically favored intermediate state produced by a concerted motion of the arsenic to liberate from dimer sites and form a "sea" of disordered arsenic on the surface. Two-dimensional clusters of arsenic and gallium appear to be distinguishable by STM. Our observations on the macroscopic evolution of the surface during annealing provides new insight into the dynamics of surface vacancies, and in connection with the adatom diffusion model of Bales and Zangwill, further insight into the nature of the equivalancy between evaporation and growth is obtained. Our observation that both unrecovered and recovered initial surfaces lead to terrace edge instabilities during annealing is somewhat surprising. It implies that the fingering patterns, which are kinetically controlled morphologies, are preferred from very different starting configurations, though they are quite unfavorable energetically. Finally, utilizing the annealing technique in a controlled way may be practically useful in surface morphology modification.

We would like to thank Professor L. M. Sander and Professor B. A. Joyce for stimulating discussions. Equipment grants from RHK Technology and Burleigh Instruments are graciously acknowledged. This work has been supported by the following grants: N00014-89-J-1519 and NSF/DMR-8857828. C.-H.L. was supported by NSF/DMR 91-17249.

*Present address: AT&T Bell laboratories, 600 Mountain Ave., Murray Hill, NJ 07974.

†Present address: Department of Mathematics, Yale University, New Haven, CT 06511.

[1]J. R. Arthur, Surf. Sci. **43**, 449 (1974).

[2]C. T. Foxon and B. A. Joyce, Surf. Sci. **50**, 434 (1975).

[3]B. G. Orr, C. W. Snyder, and M. D. Johnson, Rev. Sci. Instrum. **62**, 1400 (1991).

[4]B. G. Orr, J. Sudijono, and M. D. Johnson, in *Common Themes and Mechanisms of Epitaxial Growth,* edited by P. Fuoss, J. Tsao, D. W. Kisker, A. Zangwill, and T. Kuech, MRS Symposia Proceedings No. 312 (Materials Research Society, Pittsburgh, 1993).

[5]J. Sudijono, M. D. Johnson, C. W. Snyder, M. B. Elowitz, and B. G. Orr, Phys. Rev. Lett. **69**, 2811 (1992).

[6]J. Sudijono, M. D. Johnson, M. B. Elowitz, C. W. Snyder, and B. G. Orr, Surf. Sci. **280**, 247 (1993).

[7]E. H. C. Parker, in *The Technology and Physics of Molecular Beam Epitaxy,* edited by E. H. C. Parker (Plenum, New York, 1985).

[8]P. R. Pukite, C. S. Lent, and P. I. Cohen, Surf. Sci. **161**, 39 (1985).

[9]D. K. Biegelsen, R. D. Bringans, J. E. Northrup, and L.-E. Swartz, Phys. Rev. B **41**, 5701 (1990).

[10]A. Y. Cho, J. Appl. Phys. **47**, 2841 (1976).

[11]P. Drathen, W. Ranke, and K. Jacobi, Surf. Sci. Lett. **77**, 162 (1978).

[12]R. Z. Bachrach, R. S. Bauer, P. Chiaradia, and G. V. Hansson, J. Vac. Sci. Technol. **18**, 797 (1981).

[13]C. Deparis and J. Massies, J. Cryst. Growth **108**, 157 (1991).

[14]L. M. Sander, in *Scaling Phenomena in Disordered Systems,* edited by R. Pynn and A. Skjeltorp (Plenum, New York, 1985); D. Kessler, J. Koplick, and H. Levine, Adv. Phys. **37**, 255 (1988).

[15]W. W. Mullins and R. F. Sekerka, J. Appl. Phys. **35**, 444 (1964); R. F. Sekerka, in *Crystal Growth, an Introduction,* edited by P. Hartman (North-Holland, Amsterdam, 1973).

[16]G. S. Bales and A. Zangwill, Phys. Rev. B **41**, 5500 (1990).

[17]R. Q. Hwang, J. Schroder, C. Gunther, and R. J. Behm, Phys. Rev. Lett. **67**, 3279 (1991).

[18]B. Caroli, C. Caroli, and B. Roulet, in *Solids Far From Equilibrium,* edited by C. Godreche (Cambridge University Press, Cambridge, 1992).

[19]P. Bedrossian and T. Klitsner, Phys. Rev. Lett. **68**, 646 (1992).

[20]A. Feltz, U. Memmert, and R. J. Behm, Chem. Phys. Lett. **192**, 271 (1992).

[21]R. L. Schwoebel and E. J. Shipsey, J. Appl. Phys. **37**, 3682 (1966).

[22]M. Mundschau, E. Bauer, and W. Sweiech, Metal. Trans. A **22**, 1311 (1991); E. Bauer, M. Mundschau, W. Sweich, and W. Telieps, Ultramicroscopy **31**, 49 (1989).

[23]E. J. Heller, Z. Y. Zhang, and M. G. Lagally, Phys. Rev. Lett. **71**, 743 (1993).

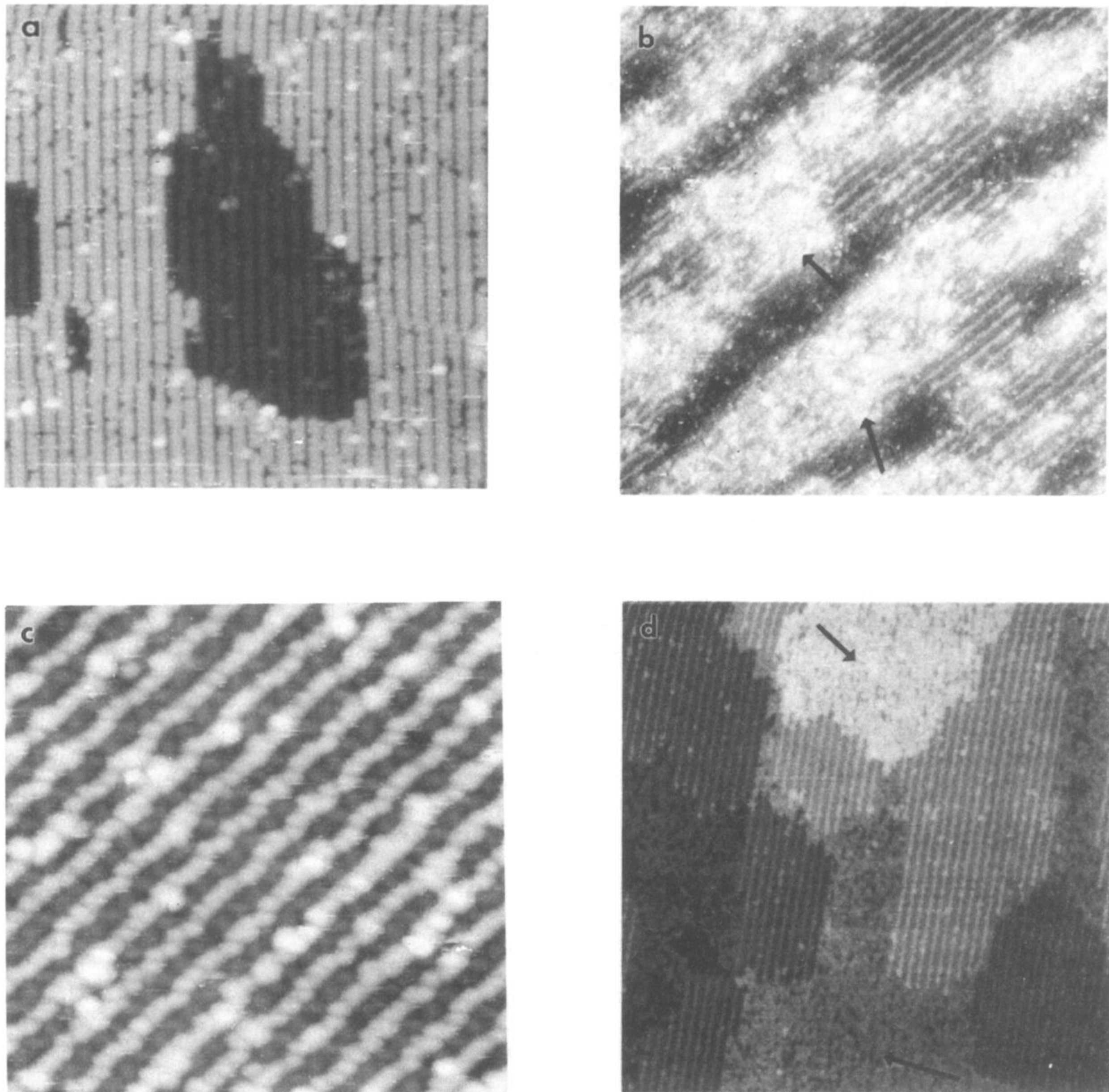

FIG. 1. Note: The orientation of the surface crystallographic directions in the figures is not necessarily the same for each figure because of rotation of the STM during the "course approach" and retraction. For all STM images, the sample bias voltage was +2.6 V and the tunneling current was 60 pA. All steps in STM images are an atomic bilayer, 0.28 nm in height. (a) High-resolution STM image of the $(2\times4)/c(2\times8)$ reconstructed GaAs(001) surface. All surfaces prior to annealing displayed this reconstruction. The scan range is 35×35 nm^2. (b) High-resolution STM image of a vacuum annealed ($T\sim480\,^{\circ}C$) surface which was quenched in the intermediate disordered state. The scan range is 60×60 nm^2. This image displays nucleation of the $\times6$ phase from the disordered surface. The atomically disordered regions (indicated by arrows) have a fuzzy texture and are believed to be made up of arsenic (i.e., arsenic clusters), while the ordered rows correspond to $\times6$ regions. (c) High-resolution STM image of the $(2\times6)/(3\times6)$ reconstructed surface. The scan range is 20×20 nm^2. (d) STM image of vacuum annealed unrecovered surface in the $(2\times6)/(3\times6)$ phase which was quenched prior to reaching the steady state fingerlike morphology. The scan range is 80×80 nm^2. The image was obtained near a ragged terrace edge and displays disordered 2D clusters absent of arsenic dimers. These 2D clusters (indicated by arrows) are believed to be Ga rich.

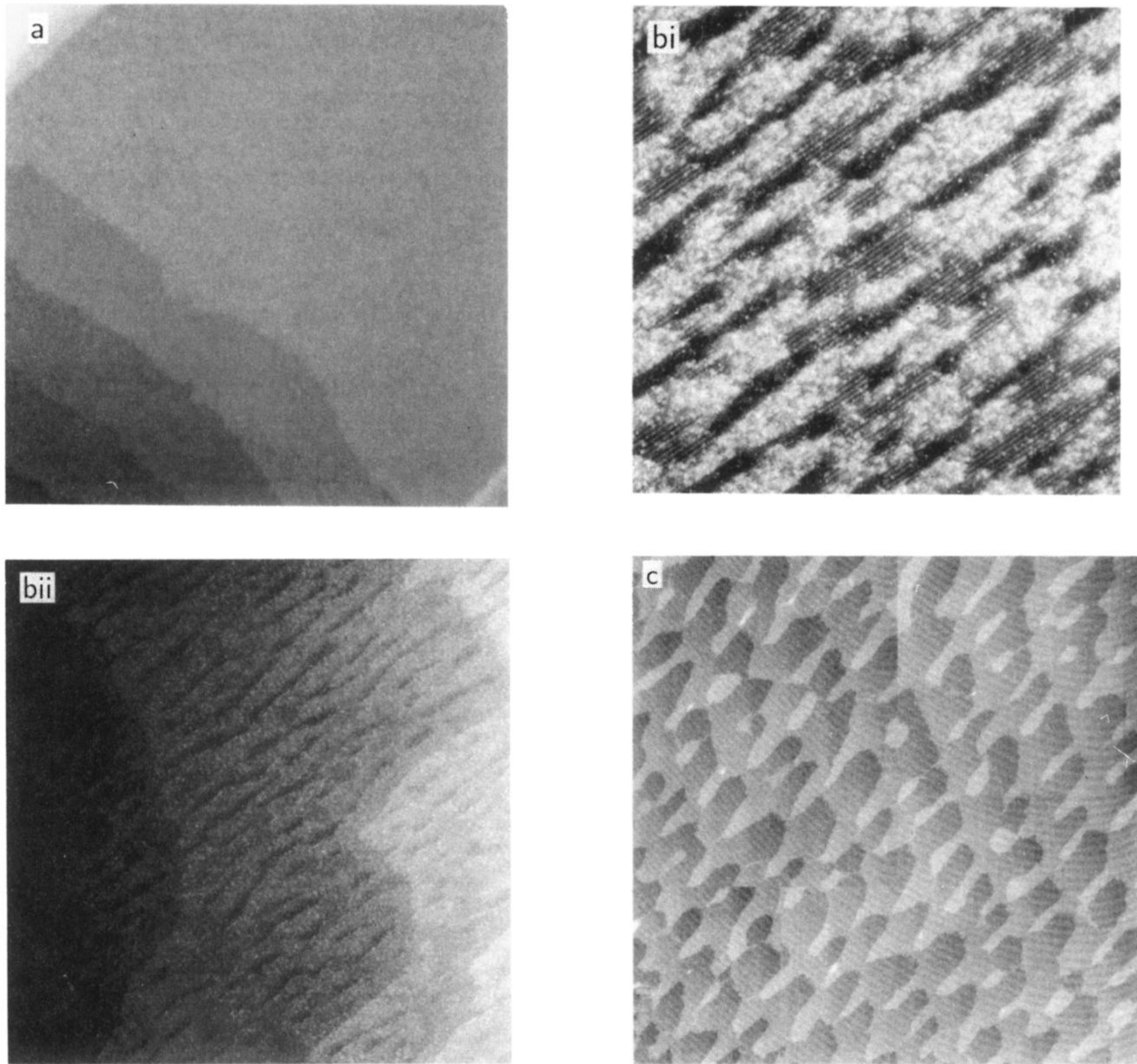

FIG. 2. (a) STM image of a recovered initial surface. The terrace edges run along the [110] direction. The scan range is 400×400 nm^2. (b) STM images after vacuum annealing a recovered surface to $\sim$480 °C and quenching in the intermediate disordered state. The scan range for the small scale image (bi) is 150×150 nm^2. The scan range for the large scale image (bii) is 400×400nm.^{2} The RHEED pattern for these surfaces was a 1×1 diffuse pattern with faint $\times6$ streaks superposed. (c) STM image of fingering patterns produced by vacuum annealing a recovered surface. The scan range is 1×1 μm^2. The fingerlike features point in the $[\bar{1}10]$ direction. The circular fringelike pattern is an artifact caused by a loose tip.

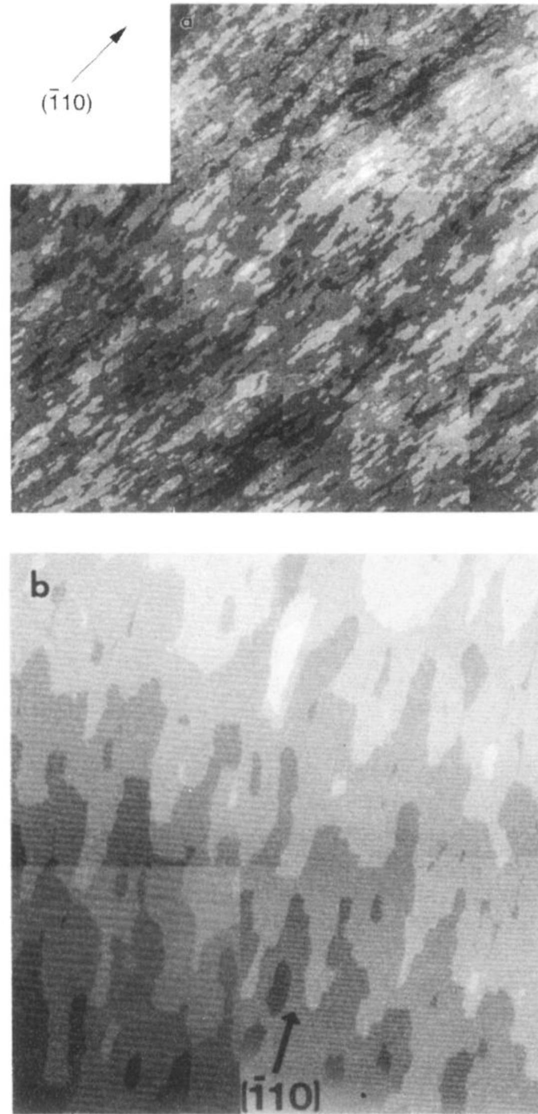

FIG. 3. (a) STM image of an unrecovered initial surface. The scan range is 600×600 nm^2. (b) STM image of fingering patterns produced by vacuum annealing an unrecovered initial surface. The scan range is 750×750 nm^2. The fringelike pattern is an artifact caused by a loose tip.

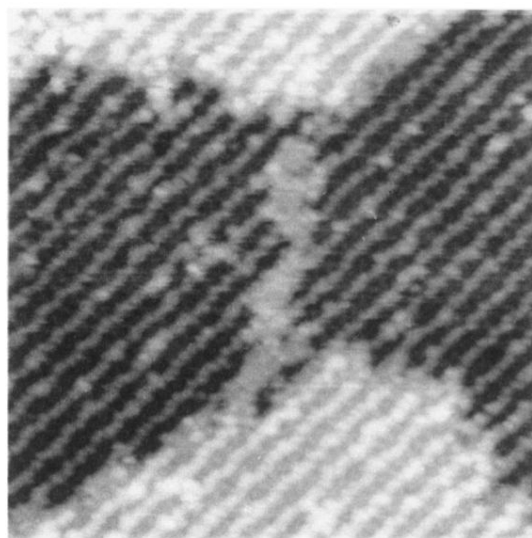

FIG. 4. STM image showing Ga coating of terrace edges on a surface displaying the fingering patterns. The scan range is 35×35 nm^2. Although, not apparent from the gray level display of the image, a measurable weight difference exists between the arsenic dimers on the lower terrace and the Ga which coats and connects the two upper terrace edges.